Micron 155 (2022) 103229

Contents lists available at ScienceDirect

Micron

journal homepage: www.elsevier.com/locate/micron

Effect of antibiotics on mechanical properties of *Bordetella pertussis* examined by atomic force microscopy

M.I. Villalba [a,b], L. Venturelli [a], L. Arnal [c], C. Masson [b], G. Dietler [a], M.E. Vela [c], O. Yantorno [b,*,1], S. Kasas [a,d,1]

[a] Laboratory of Biological Electron Microscopy (LBEM), Institute of Physics (IPHYS), Faculty of Basic Sciences (SB), Swiss Federal Institute of Technology (EPFL), and Dept. of Fundamental Biology, Faculty of Biology and Medicine, University of Lausanne (UNIL), CH-1015 Lausanne, Switzerland
[b] Centro de Investigación y Desarrollo en Fermentaciones Industriales (CINDEFI), Facultad de Ciencias Exactas, Universidad Nacional de La Plata - CONICET, 1900 La Plata, Argentina
[c] Instituto de Investigaciones Fisicoquímicas Teóricas y Aplicadas (INIFTA), Universidad Nacional de La Plata - CONICET, 1900 La Plata, Argentina
[d] Centre Universitaire Romand de Médecine Légale, UFAM, Université de Lausanne, 1015 Lausanne, Switzerland

ARTICLE INFO

Keywords:
AFM
Bordetella pertussis
Virulence
Antibiotics

ABSTRACT

In recent years, the coevolution of microorganisms with current antibiotics has increased the mechanisms of bacterial resistance, generating a major health problem worldwide. *Bordetella pertussis* is a bacterium that causes whooping cough and is capable of adopting different states of virulence, i.e. virulent or avirulent states. In this study, we explored the nanomechanical properties of both virulent and avirulent *B. pertussis* as exposed to various antibiotics. The nanomechanical studies highlighted that only virulent *B. pertussis* cells undergo a decrease in their cell elastic modulus and height upon antimicrobial exposure, whereas their avirulent counterparts remain unaffected. This study also permitted to highlight different mechanical properties of individual cells as compared to those growing in close contact with other individuals. In addition, we analyzed the presence on the bacterial cell wall of Filamentous hemagglutinin adhesin (FHA), the major attachment factor produced by virulent Bordetella spp., under different virulence conditions by Force Spectroscopy.

1. Introduction

The rapid spread of multi-drug resistant (MDR) pathogens is one of the main public health issues of the 21st century (Li and Webster, 2018; Ventola, 2015). Although the failure of antibiotic treatment was generally attributed to resistance, other mechanisms such as tolerance and persistence can also help bacteria to survive to antibiotics exposure. In addition, it is widely demonstrated that cells that are part of bacterial communities like biofilms are less susceptible to the antibiotic effects compared to those grown planktonically (Balcázar et al., 2015; Costerton et al., 1995; Donlan, 2000, 2000; Mishra et al., 2005; Patel, 2005; Singh et al., 2017).

Bordetella pertussis is a gram-negative bacterium that colonizes human airways producing pertussis or whooping cough, a highly contagious infection of the upper respiratory tract. The capacity to alternate between different virulence phases during which specific genes are expressed is characteristic of *B. pertussis*. This phenomenon known as phenotypic modulation, is depending on the environmental conditions (such as temperature or the presence or absence of modulating agents) (Deora et al., 2001; Jones et al., 2005; Merkel et al., 2003), and could be a bacterial strategy for immune evasion and persistence within the host.

Although most pathogens rapidly develop resistance to antibiotics among *Bordetella* spp. the frequency of acquired resistance to the antimicrobial agents used in clinical has been notably low. However, in the last years some reports mention the emergence of erythromycin resistance (Guillot et al., 2012; Li et al., 2019; Shahcheraghi et al., 2014). Particularly, China has experienced an increase in erythromycin-resistant *B. pertussis* isolates since they were first reported in 2013 (Liu et al., 2018; Wang et al., 2014, 2013).

Atomic force microscopy (AFM) permits to monitor bacterial adhesion, the cell wall structural dynamics, its topography as well as its mechanical properties at a nanometric scale under different

Abbreviations: AFM, Atomic Force Microscopy; FHA, Filamentous hemagglutinin adhesin; SMFS, Single Molecule Force Spectroscopy; MDR, multi-drug resistant.

* Corresponding author.
E-mail address: yantorno@quimica.unlp.edu.ar (O. Yantorno).

[1] OY and SK equal contribution.

https://doi.org/10.1016/j.micron.2022.103229
Received 31 March 2021; Received in revised form 12 December 2021; Accepted 24 January 2022
Available online 31 January 2022

environmental conditions (Abu-Lail and Camesano, 2003; Alsteens, 2012; Auer and Weibel, 2017; Dufrêne, 2014; Eaton et al., 2008; Formosa et al., 2012; Formosa-Dague et al., 2018; Hassan et al., 2019; Viljoen et al., 2020). It is therefore a very promising tool to rapidly assess the effects of antibiotics on isolated bacteria.

It is well known that some bacteria modify their roughness, height or elastic modulus (Alves et al., 2010; Laskowski et al., 2018; Longo et al., 2013; Perry et al., 2009; Pogoda et al., 2017) after exposure to antibiotics. Unfortunately, it is not known if such modifications also occur in *B. pertussis*. In this work we monitored the impacts of ampicillin and macrolides on the morphological and nanomechanical properties of *B. pertussis* in two different virulence states. Virulence states were analyzed by monitoring the presence of Filamentous hemagglutinin adhesin (FHA), -which is absent during the avirulent phase of the microorganism-, by Force Spectroscopy. We also assessed the effect of antibiotics as a function of the "social" situation of *B. pertussis*. This study highlighted striking differences between the chemical/physical properties of virulent and avirulent phenotypes. It demonstrated that isolated bacteria are more susceptible to antibiotic treatments which modify their mechanical properties than those growing in groups. This study finally confirms that the use of AFM can be a valuable tool to assess bacterial sensitivity to antibiotics in real time at a single cell level.

2. Materials and methods

2.1. Bacteria, culture conditions and AFM sample preparations

Bordetella pertussis Tohama I strain (Collection of Pasteur Institute, Paris, France -CIP8132-) and *B. pertussis* 537, a mutant strain blocked in avirulent phase derived from *B. pertussis* Tohama I, lacking the expression of the FHA protein and other virulence factors expressed on the surface and regulated by the BvgAS system (Relman et al., 1990), were used throughout this study. *B. pertussis* strains were grown in Bordet-Gengou Agar (BGA) plates supplemented with 1% w/v of Bactopectone (Difco Laboratories, Detroit, MI, USA) and 15% v/v of defibrinated sheep blood, for 48 h at 37 °C. The colonies were sub-cultured for others 48 h and then inoculated in 100 mL Erlenmeyers flaks containing 30 mL of Stainer-Scholte (SS) liquid medium adjusting the initial optical density at 650 nm (OD_{650}) to 0.20 and incubating the flasks for 24 h at 37 °C with shaking at 160 rpm. Then, the culture was centrifuged at 8000 g for 5 min and washed 4 times with sterile Phosphate-buffered saline (PBS). After that, the culture was concentrated in fresh SS liquid medium until DO_{650}: 5 in order to achieve that the bacteria cover the surface of the Petri dish (35 mm) intended for cell adhesion during AFM sample preparation process. To modulate *B. pertussis* cells from virulent phase to avirulent phase, Magnesium sulfate ($MgSO_4$) was added to 40 mM final concentration to BGA plates, as well as to cultures with SS liquid medium (Scarlato and Rappuoli, 1991). The *Escherichia coli* strains were cultivated in Luria-Bertani (LB) agar and LB broth over-night at 37 °C. Then, the cultures were centrifuged at 8000 g for 5 min and washed 4 times with sterile PBS.

2.2. Antibiotics and viability test

We used the antibiotics erythromycin (Sigma-E6376) and ampicillin (Sigma-A0166), in a concentration of 5 μg/mL and 160 μg/mL, respectively. These concentrations correspond to the minimum bactericidal concentrations that were calculated using the Antimicrobial Susceptibility Testing procedure recommended by the Clinical & Laboratory Standards Institute (CLSI) ("CLSI Publishes 2012 Antimicrobial Susceptibility Testing Standards", 2012).

The bacterial viability was checked by LIVE/DEAD® *BacLight* Bacterial Viability Kit and the mortality rates were calculated by the ratio of the surface covered by dead bacteria (red: propidium iodide) over the surface covered by all bacteria (green: SYTO9), using the software ImageJ. At least six independent samples were analyzed in the exposure to each antibiotic for each case.

2.3. Bacteria AFM sample preparations

For AFM studies, attachment of planktonic bacteria to Petri dishes (35 mm) was carried out through an adaptation of the protocol previously mentioned by Oh and Hinterdorfer (2018), using commercial 0.01% poly-L-lysine solution (PLL) (P4707, SIGMA). Initially, Petri dishes were incubated with 100 μL of PLL for 20 min at 37 °C until the surface was dried. Then 200 μL of the DO_{650}: 5 bacterial suspension was incubated on the functionalized plate for 45 min at 37 °C, it was eventually washed with sterile PBS and mounted into the AFM.

For the experiment involving grouped bacteria an inoculum of OD_{650}: 1 was incubated for 4 h in a Petri dish, (without PLL), at 37 °C in a static condition; then the culture medium was replaced with fresh medium and the culture was shacked at 160 rpm for more 4 h. Finally, the Petri dish was washed with sterile PBS and inserted into the AFM equipment.

2.4. Sample preparation for protein-antibody interaction

A freshly cleaved mica disc was used as substrate for these experiments. It was functionalized with 50 μL 1% 3-aminopropyltriethoxysilane (APTES) ethanolic solution for 1 min and washed three times with Milli-Q water. Eventually the mica was dried under N_2 and incubated with a 0.5% glutaraldehyde (GA) aqueous solution for 15 min. A new wash with Milli-Q water and drying with N_2 was carried out. The mica disks were incubated for 15 min in 30 μL of a 10 ng/μL purified FHA solution (Sigma, St. Louis, MO, USA) diluted in a PBS buffer. As a control we performed an antibody blocking experiments in which the FHA functionalized mica disks were incubated with an anti-FHA monoclonal antibody (NIBSC, London, England) solution (10 ng/μL) for 1 h before performing the force spectroscopy experiments.

2.5. Functionalization of cantilever with antibodies

For these experiments we used silicon nitride (DNP-10, Bruker) triangular cantilevers with a nominal spring constant of 0.06 N/m -range: 0.03 N/m and 0.12 N/m (DNP-D)-. Their spring constant was calibrated by the thermal noise method.

The functionalization of the cantilever was carried out by incubation with an aqueous solution of 0.05% w/v GA for 15 min, followed by three washes with ultrapure water and an incubation with the anti-FHA solution (70 ng/μL) for 30 min at room temperature (Arnal et al., 2015). Finally, the probe was washed with sterile PBS and mounted on the AFM tip holder.

2.6. Single molecule Force Spectroscopy (SMFS)

Data acquisition of the antigen-antibody interaction was performed using a JPK NanoWizard III (JPK Instruments, Bruker, Germany). Interaction measurements between protein and antibody were recorded in a PBS buffer. The maximum force applied was 1 nN and the Z length was 0.5 μm. 500 force curves were acquired for each retraction speed analyzed (50, 100, 500 and 1000 nm/s), keeping the contact time on the surface at 500 ms. The loading rate (ld) was calculated as the product of the retraction speed and the force constant of the cantilever (Xu and Siedlecki, 2009; Lee et al., 2006).

Data acquisition of the bacterium-antibody interaction was taken from bacteria attached by PLL in the bottom of a Petri dish, as mentioned before, incubated in SS culture medium at room temperature. For each case were analyzed at least 3 individual bacteria from independent cultures and experiments. For each bacterium analyzed, 30 force curves were acquired before and after a period of 5 h. The force curves were recorded in the direction perpendicular to the surface with a Z length of 1000 nm and duration of 5 s for each stage, including an intermediate

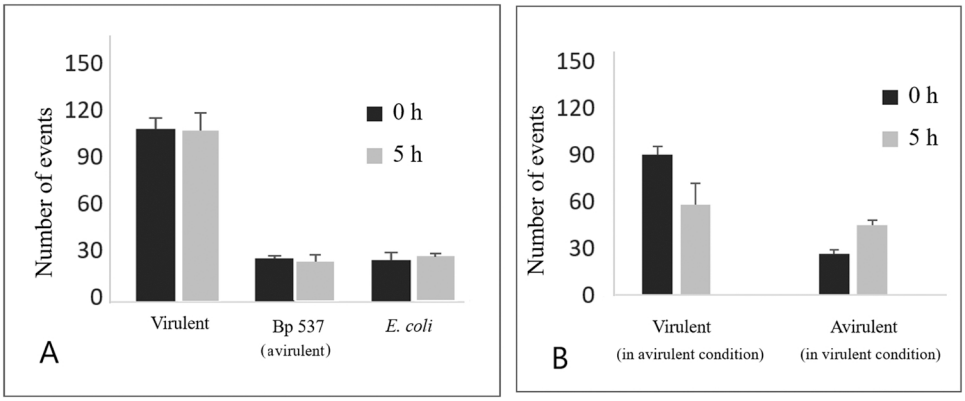

Fig. 1. A) Number of adhesion events between a cantilever functionalized with anti-FHA and *B. pertussis* cells: virulent and avirulent. The interaction was also analyzed over *E. coli* bacteria taken as a negative control. B) Number of adhesion events *B. pertussis* Tohama I – anti-FHA on virulent bacteria incubated during the data acquisition in 40 mM $MgSO_4$, (conditions that induce a change towards the avirulent state), -"Virulent (in avirulent condition"), it means-. On the contrary, - "Avirulent (in virulent condition)"-, represents an analysis of *B. pertussis* Tohama I avirulent bacteria (from over-night culture supplemented with $MgSO_4$) under conditions that induce virulence, it means that the experiment begins with avirulent bacteria that are incubated for 5 h in a medium without the presence of $MgSO_4$. In this environmental condition bacteria are induced to change its avirulent state towards the virulent one. Error bars represent the standard error.

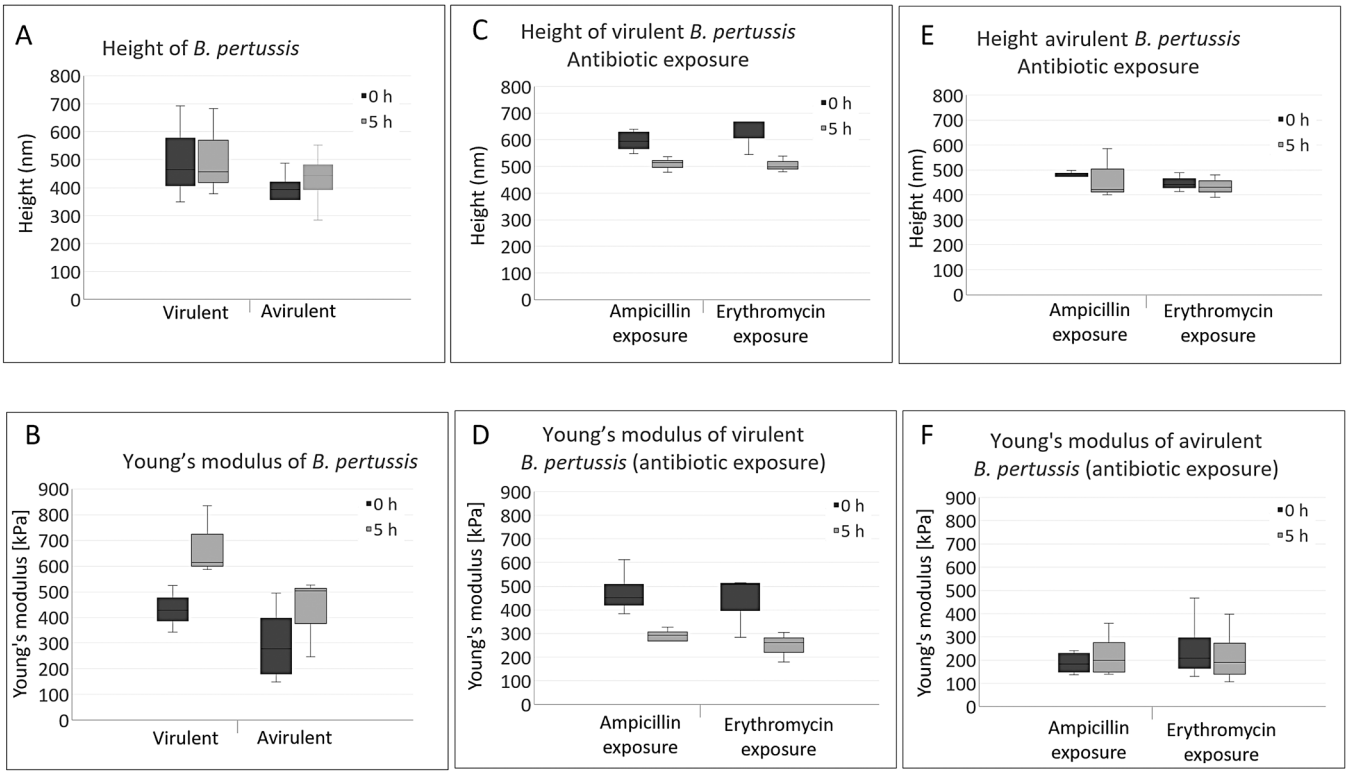

Fig. 2. Mechanical properties of *B. pertussis*. A) Height and (B) Young's modulus of virulent *B. Pertussis* Tohama I strain and avirulent *B. pertussis* 537 strain. (C) Height and (D) Young's modulus of virulent *B. pertussis* Tohama I strain before and after antibiotic exposure. (E) Height and (F) Young's modulus of avirulent *B. pertussis* 537 strain before and after antibiotic exposure. All the force curves were used as a single population to build the boxplot (number of cells: at least 3 for each mean value).

pause at the surface (also 5 s). We noticed that the concentration of the protein was much higher on the mica surface than on virulent bacteria, therefore a pause of 5 s permitted to increase the chances to observe binding-unbinding events. In cases where it was desired to follow the virulence change, 40 mM $MgSO_4$ solution was added to the SS medium of the Petri dish where bacteria are located and the data recording was carried out.

Finally, the data analysis was carried out using the JPK Data Processing software (Version spm-5.1.4). The number of antigen-antibody interactions was counted manually. The average number of events for 3 bacteria was considered. Only interaction events with specific values that correspond to an antigen-antibody interaction (range between 50 pN and 900 pN) (Arnal et al., 2015; Moreno et al., 2011; Schwesinger et al., 2000) were considered.

2.7. Nanomechanical properties analysis of individual B. pertussis cells

For these experiments we used a NanoWizard III microscope (JPK Instruments, Bruker, Germany) equipped with triangular silicon nitride cantilevers with a nominal spring constant of 0.06 N/m – range: 0.03 N/m and 0.12 N/m (DNP-D). Data collection was carried out at room temperature using the Quantitative Image (QI) mode. Typical topographic images of 2 × 2 or 2.5 × 2.5 μm^2 were taken for individual bacteria with a setpoint force of 1 nN (number of pixels: 64 × 64 or 128

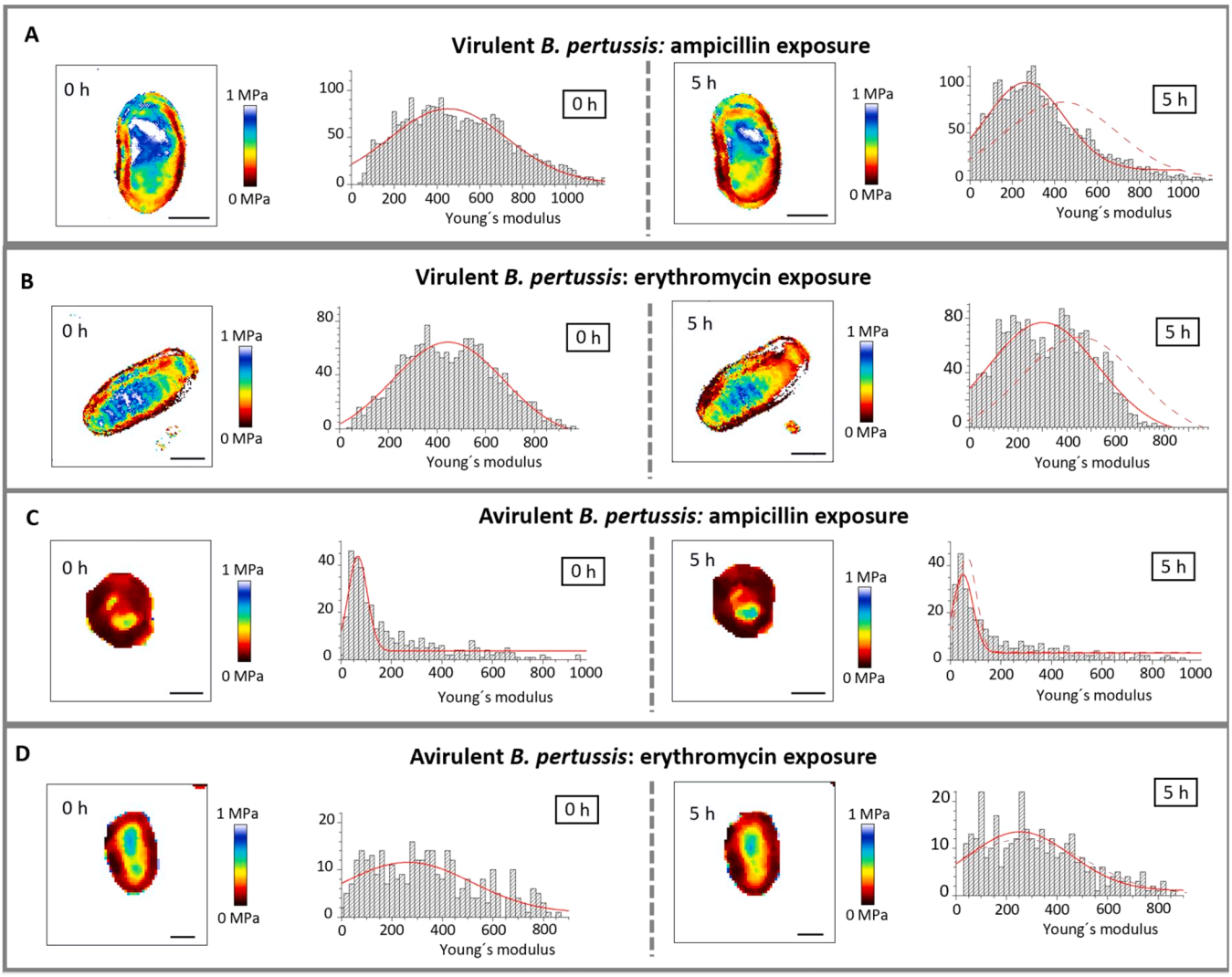

Fig. 3. Elasticity images and their respective Youngś modulus histograms of virulent *B. pertussis* cells before and after (0 h: left and 5 h: right) (A) ampicillin and (B) erythromycin exposure. C) and D) represent the elasticity image and their respective Youngś modulus histograms of avirulent *B. pertussis* cells before and after (5 h) ampicillin and erythromycin exposure respectively. Dash line in 5 h histograms represent curves fit of the same bacterium at 0 h. Blue-white represents high and brown low elastic modulus values. Bacteria are attached to the Petri dish by 0.01% poly-L-lysine solution. Scale bar: 500 nm.

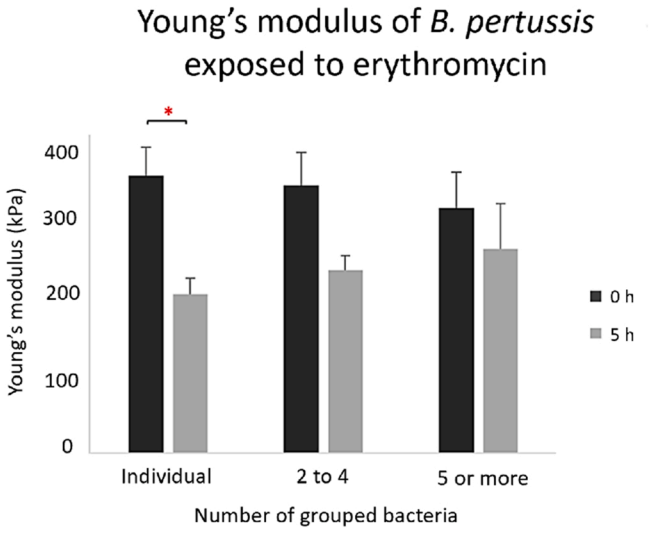

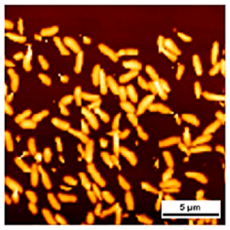

Fig. 4. Left: Elasticity of virulent *B. pertussis* before and after antibiotic exposure according to the number of bacteria being part of the group and a representative height image (*represents significative differences, Student's t-test: $\alpha = 0.05$). Right: Height images of grouped and isolated bacteria in the same AFM field. *B. pertussis* cells were attached by a static incubation in Petri dish during 4 h followed of 4 h under shaking with fresh medium.At least 5 individual cells in each situation were analyzed. Error bars represent the standards errors.

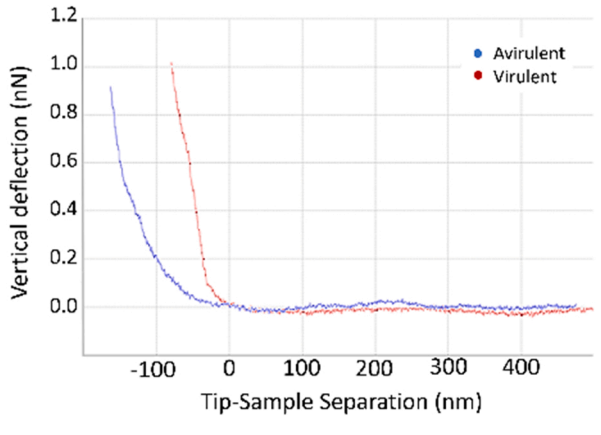

Fig. A1. A) AFM curves: vertical deflection vs Tip-sample separation of virulent *B. pertussis* Tohama I and avirulent mutant *B.* pertussis 537. B) Force vs indentation curves of virulent and avirulent *B. pertussis*.

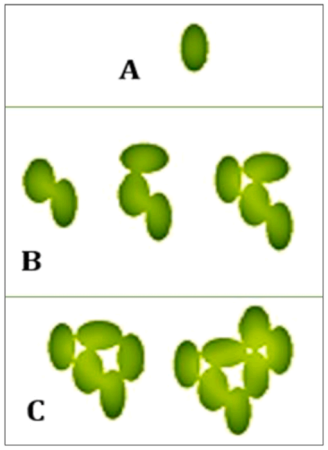

Fig. A2. Schematic representation of the analysis categories of each bacterium according to the number of bacteria that are part of the cell group to which they belong: A) individual bacteria, B) 2–4, and C) 5 or more grouped bacteria.

× 128). The data of clustered bacteria were acquired in QI from 6 × 6 and 10 × 10 μm^2 images (typical AFM curves of virulent and avirulent *B. pertussis* are shown in Fig. A1).

The root mean square (RMS) roughness (Alves et al., 2010) was measured for each individual cell. Topographic images (contact point topographies) were flattened using zero order off set to remove the scan line misalignment, the contact point reconstructed topographies have been used for calculate this parameter. For each bacteria RMS was measured in at least three different center areas with fixed size of 140 × 140 nm^2 over three or more bacteria in each condition. Bacteria heights were quantified using the software JPK Data Processing. The mean Young's modulus (E) was estimated individually for each bacterium based on the curves recorded according to the Hertz-Sneddon model applied to force-indentation curves (Eq. (A1)) (Arnal et al., 2012; Dewan et al., 2018). The Sneddon fit was done on the whole indentation. For the

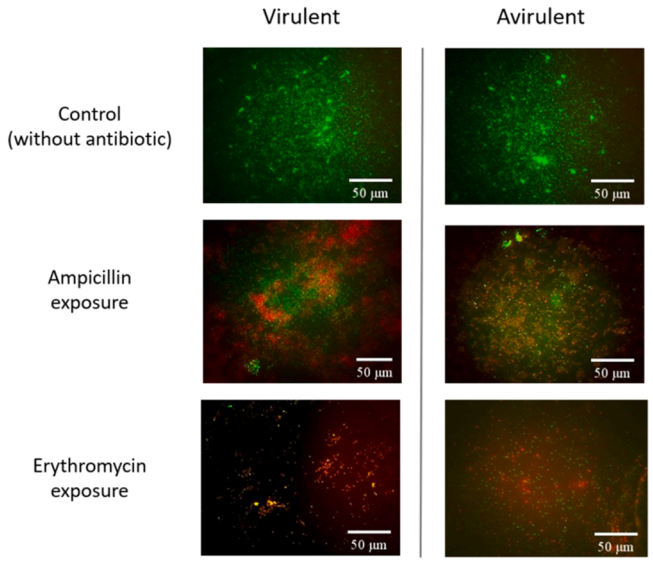

Fig. A4. Fluorescence microscopy images of *B. pertussis* cells attached to a Petri dish with 0.01% poly-L-lysine solution after 5 h of antibiotics exposure in virulent and avirulent phases. Staining: PI-SYTO9 (green: live and dead bacteria; red: only dead).

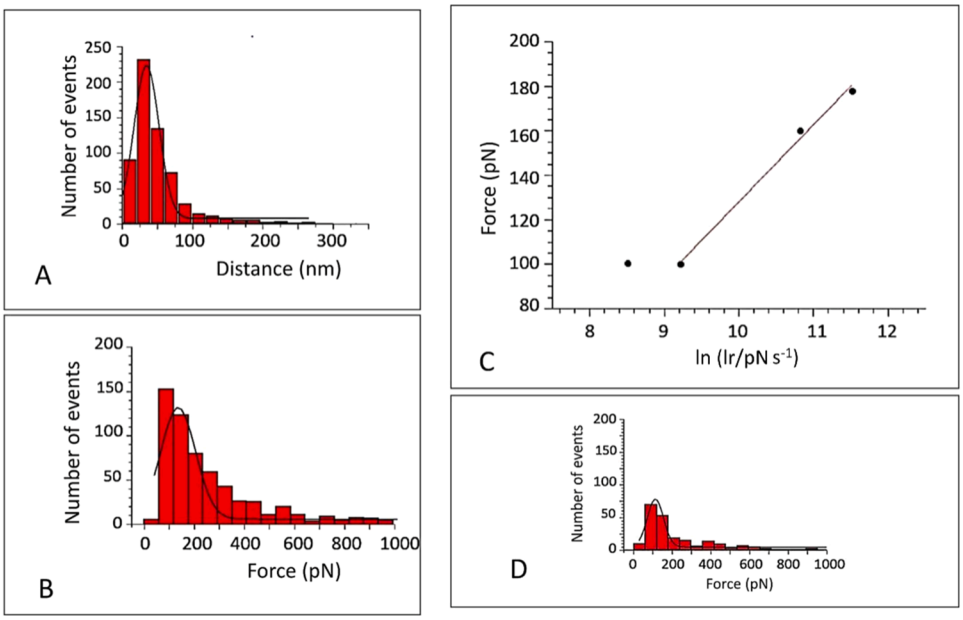

Fig. A3. (A) Histogram of the distance values between the contact point and the interaction event found at the speed of 500 nm/s. (B) Histogram of the distribution of forces recorded at a speed of 500 nm/s on FHA sample. (C) Relationship of the mean interaction force for the 4 values of loading rate that were tested. Two different segments are observed, the segment determined by the last three points was fitted with a linear function, (linear adjustment with a R2 value: 0.92). The speed selected for the studies corresponds to one of the intermediate values of that linear segment. (D) Histogram of the distribution of forces recorded at a speed of 500 nm/s on FHA sample after blocked with anti-FHA purified.

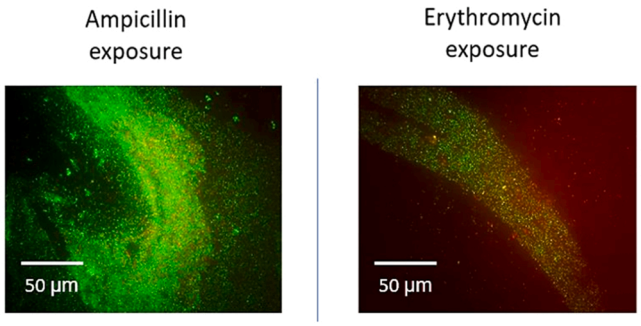

Fig. A5. Fluorescence microscopy images of grouped *B. pertussis* (virulent phase), (attached to a Petri dish by static 4 h incubation followed by of a shaking 4 h incubation), after 5 h of antibiotics exposure. Staining: PI-SYTO9 (green: live and dead bacteria; red: only dead).

Table A1
Rates of bacterial mortality of individual *B. pertussis*, dead bacteria over total bacteria, acquired from LIVE/DEAD images analysis (Fig. A4), after 5 h of antibiotic treatment. Cells were attached to a Petri dish with 0.01% poly-L-lysine solution. No significant differences between mortality rates of avirulent and virulent were detected (*t-test* $P > 0.05$).

Phase	*Not antibiotic*	*Ampicillin exposure*	*Erythromycin exposure*
Avirulent	0.008 (± 0.002)	0.78 (± 0.03)	0.58 (± 0.17)
Virulent	0.003 (± 0.0009)	0.85 (± 0.06)	0.79 (± 0.12)

Table A2
RMS Roughness mean values acquired by JPK Data processing software, for virulent and avirulent *B. pertussis* attached to Petri dish with 0.01% poly-L-lysine solution, before and after 5 h of antibiotic exposures. No significant differences between RMS values (*t-test* $P > 0.05$).

Exposure time	Virulent		Avirulent	
	Ampicillin	*Erythromycin*	*Ampicillin*	*Erythromycin*
0 h	9.59 (± 0.77)	10.53 (± 0.78)	10.33 (± 0.55)	11.17 (± 1.25)
5 h	9.67 (± 0.95)	9.41 (± 0.52)	10.82 (± 1.25)	10.49 (± 1.62)

Table A3
Rates of mortality, (dead bacteria over total bacteria), of grouped virulent *B. pertussis,* acquired from LIVE/DEAD images analysis (Fig. A4), after 5 h of antibiotic treatment. Bacteria were attached to a Petri dish by static 4 h incubation follow of a shaking 4 h incubation. No significant differences between mortality rates were detected (*t-test* $P > 0.05$).

Control (without antibiotic)	*Ampicillin exposure*	*Erythromycin exposure*
0.0025 (± 0.0002)	0.011 (± 0.0070)	0.025 (± 0.0080)

study of elastic modulus in grouped bacteria, each cell was selected and evaluated considering the number of bacteria that are in contact with it or are part of the bacterial group/cluster. In this way, Young's modulus (E) of individual bacteria was studied comparatively in three different situations: i) individual bacterium, ii) bacterium being part of a group formed by 2–4 cells and iii) bacterium being part of a group formed by 5 or more cells (Fig. A2). These properties were tested before and after of exposure to each antibiotic. The first QI was taken at the time considered as initial time: 0 h. Next, the antibiotic was added to the Petri dish where the cells were attached. After 5 h of incubation with each antibiotic a new QI was taken over the same imaging field preserving the acquisition parameter and the probe.

JPK data processing software, Origin and MatLab 2013 were used to process the data. An average of 1500 curves per each bacterium was analyzed. The final results were represented as a mean ± standard error, at least 4 different cells from 3 replicates cultures were analyzed in each condition. The statistical significance was assessed using Student's t-test ($\alpha = 0.05$).

3. Results

B. pertussis express different membrane proteins in each virulence phase. For example Filamentous hemagglutinin adhesin (FHA) is a fundamental protein in the adhesion process for virulent phase, but it is non-expressed in avirulent phase (Jones et al., 2005; Relman et al., 1990). The expression of FHA was analyzed before and after incubation of cells under different culture conditions that induce changes in virulence phase by using single molecule Force Spectroscopy. As an initial step, an analysis of the interaction between the commercial monoclonal anti-FHA antibody and the purified FHA protein on mica was performed. The ramp velocity was set to 500 nm/s. The statistical median of the distribution of interaction forces and the mean value of the distance from the point of contact recorded at this retraction speed were ~ 160 pN and 38.79 nm, respectively (Fig. A3). These values are within the range of values reported for antigen-antibody interactions (Arnal et al., 2015; Dewan et al., 2018; Ido et al., 2014; Kajava et al., 2001; Moreno et al., 2011; Schwesinger et al., 2000).

An analysis of interaction between bacteria and monoclonal antibody anti-FHA was done to analyze the virulence state. Our results showed that in bacteria blocked in avirulent phase (Bp 537) the number of adhesion events between FHA and anti-FHA is the smallest and has not significative difference with the number of adhesion events registered over *E. coli* (as a control having no FHA on its surface). *B. pertussis* Tohama I virulent strain has the highest number or adhesion events, which means that bacteria in virulent phase express extensively this adhesin (Fig. 1A). This is in agreement with the work previously published by Arnal et al. (2012). The analysis of the bacteria in an environment that induces a virulence variation suggests that FHA expression changes under these conditions ("virulent bacterium in avirulent condition" and "avirulent in virulent condition") (Fig. 1B). Counting the number of binding-unbinding events permitted to determine the virulence status of the bacteria and then to correlate it to their mechanical properties.

Virulent and avirulent *B. pertussis* cells exposed to two antibiotics with different effects on these bacteria were analyzed after 5 h exposition. The rates of bacterial mortality calculated for each treatment using LIVE/DEAD stain are not significantly different between virulence states (Fig. A4 and Table A1). The analyzes of the topography of *B. pertussis* single cells of each phenotype exposed to antibiotics revealed no significant changes in the surface roughness for virulent and avirulent phases (Table A2). However, with higher resolution the topography at the molecular level would have shown a different result. These results are consistent with the poor efficiency of ampicillin over the thin layer of peptidoglycan of gram-negative bacteria, and with the mechanism of action of erythromycin: it acts on protein synthesis but does not affect the outer membrane roughness of bacteria.

The analysis of the morphological properties of *B. pertussis* after the treatment with ampicillin and erythromycin showed a significative decrease in the height of virulent bacteria as well as a shift in the Young's modulus towards lower values (Figs. 2 and 3). However, when carrying out the same experiment in avirulent *B. pertussis* no changes in height and Young's modulus after antimicrobial exposure could be observed. The significant difference between Young modulus and height of virulent and avirulent bacteria could be related to a mechanism of better adaptation of the avirulent bacteria to the presence of antibiotics as it was shown in *B. bronchiseptica* where antibiotic-resistant mutants are associated with the loss of virulence (Dewan et al., 2018).

It is well known that bacteria in clusters behave differently towards antibiotics than their isolated counterparts. Numerous hypothesis can

explain this phenomenon, among those we can cite some as the inability of the antibiotic to penetrate the cellular groups, the existence of microenvironments that antagonize the action of antibiotics, the activation of stress responses that cause changes in the physiology of the bacteria, or the appearance of a specific phenotype that actively combats the negative effects of antimicrobial substances (Singh et al., 2017; Stewart, 2002). However, very little is known about the nanomechanical properties of *B. pertussis* growing in clusters and their differences with individual isolates. In this part of the study, we measured the mechanical properties of individual and grouped cells and explored the dependence of their mechanical properties as a function of their neighborhood, i.e. the number of bacteria or size of the group to which they belong.

As depicted in Fig. 4, changes in elasticity of isolated bacteria exposed to antibiotic are more pronounced than for those that are living in groups. Bacteria being part of a group of 5 or more cells has smaller changes of elastic modulus-elasticity than isolated ones. This observation of a cluster of few bacteria is consistent with the smaller mortality rates registered to grouped bacteria (Fig. A5 and Table A3) and the well-known tolerance of grouped bacteria against antimicrobials.

4. Discussion

Many works have studied the mechanical properties of individual bacteria under different environmental conditions focusing on the properties of cells surface and their behavior under stress conditions. Gaboriaud et al. (2005) investigated the nanomechanical properties of gram-negative bacillus *Shewanella putrefaciens* in aqueous solutions and observed that an increase in the pH of the culture medium causes an increase in cell height and a decrease in elasticity of the surface polymeric layer. Longo et al. (2013) characterized the mechanical properties of the outer membrane of *E. coli* and reported that the membrane has more rigid areas possibly associated with the intracellular structure. Bacterial cells may show significant local variations in elasticity due to the complex composition of their cell wall (Touhami et al., 2003).

The mean values of Young's modulus of *B. pertussis* obtained in this work are similar with those previously reported (Arnal et al., 2012), as well as for other bacteria such as *Staphylococcus aureus* (Perry et al., 2009) or *E. coli* (Longo et al., 2012). However, a specific software to exclude the boundary pixels could give a more robust estimation. Arnal et al. (2015) associated, in *B. pertussis,* the elastic modulus with presence of the outer membrane adhesin FHA, which is essential for adhesion to epithelial cells. Based on this and ours results, we can suggest that changes in the virulence phase and concomitantly the variation in the expression of outer membrane proteins affect the nanomechanical properties of cell cover. The phase variation process consists of a change in the expression of surface proteins and specific virulence factors as result of monitoring the physicochemical conditions of the environment that the pathogen is capable make in a specific niche. Overall nanomechanical properties of the bacterial surface during this adaptation can be quantified using atomic force microscopy.

In the case of *B. pertussis* the virulence changes during the adaptation of the bacterium to the host environment represent a very important process for the understanding of the pertussis infection which could be analyzed by a nanoscale study. It has been important here to be able to determine differences in the level of cell cover elasticity between the virulence phases. This characteristic could be related to adhesion and infection capacity considering that FHA is a fundamental and specific virulence's adhesin. It suggests that there is a correlation between FHA expression and the increase in Young's modulus, but it is important to consider that other causes could affect this mechanical property.

Also, nanoindentation has been used to demonstrate the effect of antimicrobial agents on the cell wall of bacteria as well as to evaluate mechanisms of action of new antimicrobial agents on the cell wall of resistant strains (Gaveau et al., 2017). Several studies showed that bacteria treated with antibiotics have a lower Young's modulus than untreated ones (Eaton et al., 2008; Gaboriaud et al., 2005; Gaveau et al., 2017; Pogoda et al., 2017); that is, antimicrobial agents generate a softening of bacterial cell walls. In this work we observe the reduction in the elasticity of the virulent bacterial outer membrane (in this case of gram-negative bacteria) due to exposure to antibiotics, coinciding with previous works (Longo et al., 2013; Touhami et al., 2003). The changes can be attributed to the inhibition of the bridges between peptidoglycan and PBP (penicillin-binding proteins) by the ampicillin (a beta-lactam, interferes with the synthesis of the bacterial cell wall), and the restricted protein synthesis by erythromycin (it acts at the ribosomal level inhibiting the synthesis of proteins). It has been demonstrated that incubation of bacteria with macrolides decreases the adhesion capacity of *B. pertussis* to epithelial cells (Scaglione et al., 1994). Previously, it has been shown that the adoption of an avirulent state generates significant metabolic and gene expression changes that may be participating in bacterial survival, transmission, and/or persistence (Karataev et al., 2016; Moon et al., 2017). An alternative explanation to the observed behavior would be differences in the turgor pressure between virulent and avirulent phenotypes. If we suppose that avirulent cells are less turgid, a treatment reducing their internal pressure would have a stronger effect on more pressurized bacteria than on already loose ones. The differences observed in height between virulent and avirulent phenotypes and its variation after antibiotic exposure, may support this hypothesis. Grouped *B. pertussis* cells, in the short period of time of analysis (5 h), demonstrated different response to the action of the antibiotics tested. This way of life in groups allowed detecting a lower percentage of elasticity decrease in the elastic modulus after treatment with antimicrobials in cells that are part of these bacterial clusters with respect to cells that are isolated.

5. Conclusions

In this study we explored by using AFM mechanical properties of virulent and avirulent *B. pertussis* cells before and after exposure to antibiotics. The study revealed significant differences in the surface properties of virulent and avirulent phenotypes and highlighted different mechanical responses of the two phenotypes to antibiotics. It also revealed that grouped bacteria react differently than isolated ones. In general, these results confirm the usefulness of AFM to study microorganisms and their reaction to different physic-chemical stimulus with unpreceded spacial and temporal resolution.

Declaration of Competing Interest

The authors declare that they have no known competing financial interests or personal relationships that could have appeared to influence the work reported in this paper.

Funding and Acknowledgments

Swiss members of the team were funded by the Swiss National Science Foundation 200021-144321, 310030L_197946, CRSII5_173863 and 407240_167137. MIV was supported by Swiss Government Excellence Schol-arships (ESKAS-Nr:2018.0647) and CONICET. MEV is a member of the research career of CIC PBAand was funded by ANPCyT (Argentina, PICT:2016-0679) and CONICET PUE 22920170100100CO. OY was supported by ANPCyT (Argentina, PICT 2017-2444).

Appendix A

A.1. Young modulus–Hertz-Sneddon model

The theoretical model considers the shape of the probing tip, there the tip was modeled as a pyramidal-cone, thus, the relation between load force F and indentation depths δ is:

$$F = \frac{2}{\pi(1-\nu^2)} E \tan\alpha \, \delta^2 \tag{A1}$$

where α: the open angle of the probing tip, in our case 18°, E: E is the Young's modulus of the sample and ν is the Poisson's ratio of the sample (assumed as 0.5 for cells).

A.2. Figures and tables

See Figs. A1–A5.

A.3. Tables

See Tables A1–A3.

References

Abu-Lail, N.I., Camesano, T.A., 2003. Role of ionic strength on the relationship of biopolymer conformation, DLVO contributions, and steric interactions to bioadhesion of Pseudomonas putida KT2442. Biomacromolecules 4, 1000–1012. https://doi.org/10.1021/bm034055f.

Alsteens, D., 2012. Microbial cells analysis by atomic force microscopy. Methods Enzym. 506, 3–17. https://doi.org/10.1016/B978-0-12-391856-7.00025-1.

Alves, C.S., Melo, M.N., Franquelim, H.G., Ferre, R., Planas, M., Feliu, L., Bardají, E., Kowalczyk, W., Andreu, D., Santos, N.C., Fernandes, M.X., Castanho, M.A.R.B., 2010. Escherichia coli cell surface perturbation and disruption induced by antimicrobial peptides BP100 and pepR. J. Biol. Chem. 285, 27536–27544. https://doi.org/10.1074/jbc.M110.130955.

Arnal, L., Longo, G., Stupar, P., Castez, M.F., Cattelan, N., Salvarezza, R.C., Yantorno, O. M., Kasas, S., Vela, M.E., 2015. Localization of adhesins on the surface of a pathogenic bacterial envelope through atomic force microscopy. Nanoscale 7, 17563–17572. https://doi.org/10.1039/c5nr04644k.

Arnal, L., Serra, D.O., Cattelan, N., Castez, M.F., Vázquez, L., Salvarezza, R.C., Yantorno, O.M., Vela, M.E., 2012. Adhesin contribution to nanomechanical properties of the virulent Bordetella pertussis envelope. Langmuir 28, 7461–7469. https://doi.org/10.1021/la300811m.

Auer, G.K., Weibel, D.B., 2017. Bacterial cell mechanics. Biochemistry 56, 3710–3724. https://doi.org/10.1021/acs.biochem.7b00346.

Balcázar, J.L., Subirats, J., Borrego, C.M., 2015. The role of biofilms as environmental reservoirs of antibiotic resistance. Front. Microbiol. 6, 1216. https://doi.org/10.3389/fmicb.2015.01216.

CLSI Publishes 2012 Antimicrobial Susceptibility Testing Standards [WWW Document], 2012. Medical Design and Outsourcing. ⟨https://www.medicaldesignandoutsourcing.com/clsi-publishes-2012-antimicrobial-susceptibility-testing-standards/⟩, (Accessed 31 March 2021).

Costerton, J.W., Lewandowski, Z., Caldwell, D.E., Korber, D.R., Lappin-Scott, H.M., 1995. Microbial biofilms. Annu. Rev. Microbiol. 49, 711–745. https://doi.org/10.1146/annurev.mi.49.100195.003431.

Deora, R., Bootsma, H.J., Miller, J.F., Cotter, P.A., 2001. Diversity in the Bordetella virulence regulon: transcriptional control of a Bvg-intermediate phase gene. Mol. Microbiol. 40, 669–683. https://doi.org/10.1046/j.1365-2958.2001.02415.x.

Dewan, K.K., Skarlupka, A.L., Rivera, I., Cuff, L.E., Gestal, M.C., Taylor-Mulneix, D.L., Wagner, S., Ryman, V.E., Rodriguez, C., Hamidou Soumana, I., Levin, B.R., Harvill, E.T., 2018. Development of macrolide resistance in Bordetella bronchiseptica is associated with the loss of virulence. J. Antimicrob. Chemother. 73, 2797–2805. https://doi.org/10.1093/jac/dky264.

Donlan, R.M., 2000. Role of biofilms in antimicrobial resistance. ASAIO J. 46, S47–S52. https://doi.org/10.1097/00002480-200011000-00037.

Dufrêne, Y.F., 2014. Atomic force microscopy in microbiology: new structural and functional insights into the microbial cell surface. mBio 5. https://doi.org/10.1128/mBio.01363-14 (e01363-01314).

Eaton, P., Fernandes, J.C., Pereira, E., Pintado, M.E., Xavier Malcata, F., 2008. Atomic force microscopy study of the antibacterial effects of chitosans on Escherichia coli and Staphylococcus aureus. Ultramicroscopy 108, 1128–1134. https://doi.org/10.1016/j.ultramic.2008.04.015.

Formosa, C., Grare, M., Jauvert, E., Coutable, A., Regnouf-de-Vains, J.B., Mourer, M., Duval, R.E., Dague, E., 2012. Nanoscale analysis of the effects of antibiotics and CX1 on a Pseudomonas aeruginosa multidrug-resistant strain. Sci. Rep. 2, 575. https://doi.org/10.1038/srep00575.

Formosa-Dague, C., Duval, R.E., Dague, E., 2018. Cell biology of microbes and pharmacology of antimicrobial drugs explored by Atomic Force Microscopy. Semin. Cell Dev. Biol. 73, 165–176. https://doi.org/10.1016/j.semcdb.2017.06.022.

Gaboriaud, F., Bailet, S., Dague, E., Jorand, F., 2005. Surface structure and nanomechanical properties of Shewanella putrefaciens bacteria at two pH values (4 and 10) determined by atomic force microscopy. J. Bacteriol. 187, 3864–3868. https://doi.org/10.1128/JB.187.11.3864-3868.2005.

Gaveau, A., Coetsier, C., Roques, C., Bacchin, P., Dague, E., Causserand, C., 2017. Bacteria transfer by deformation through microfiltration membrane. J. Membr. Sci. 523, 446–455. https://doi.org/10.1016/j.memsci.2016.10.023.

Guillot, S., Descours, G., Gillet, Y., Etienne, J., Floret, D., Guiso, N., 2012. Macrolide-resistant Bordetella pertussis infection in newborn girl, France. Emerg. Infect. Dis. 18, 966–968. https://doi.org/10.3201/eid1806.120091.

Hassan, A.A., Vitorino, M.V., Robalo, T., Rodrigues, M.S., Sá-Correia, I., 2019. Variation of Burkholderia cenocepacia cell wall morphology and mechanical properties during cystic fibrosis lung infection, assessed by atomic force microscopy. Sci. Rep. 9, 16118. https://doi.org/10.1038/s41598-019-52604-9.

Ido, S., Kimiya, H., Kobayashi, K., Kominami, H., Matsushige, K., Yamada, H., 2014. Immunoactive two-dimensional self-assembly of monoclonal antibodies in aqueous solution revealed by atomic force microscopy. Nat. Mater. 13, 264–270. https://doi.org/10.1038/nmat3847.

Jones, A.M., Boucher, P.E., Williams, C.L., Stibitz, S., Cotter, P.A., 2005. Role of BvgA phosphorylation and DNA binding affinity in control of Bvg-mediated phenotypic phase transition in Bordetella pertussis. Mol. Microbiol. 58, 700–713. https://doi.org/10.1111/j.1365-2958.2005.04875.x.

Kajava, A.V., Cheng, N., Cleaver, R., Kessel, M., Simon, M.N., Willery, E., Jacob-Dubuisson, F., Locht, C., Steven, A.C., 2001. Beta-helix model for the filamentous haemagglutinin adhesin of Bordetella pertussis and related bacterial secretory proteins. Mol. Microbiol. 42, 279–292. https://doi.org/10.1046/j.1365-2958.2001.02598.x.

Karataev, G.I., Sinyashina, L.N., Medkova, A.Y., Semin, E.G., Shevtsova, Z.V., Matua, A. Z., Kondzariya, I.G., Amichba, A.A., Kubrava, D.T., Mikvabia, Z.Y., 2016. Insertional inactivation of virulence operon in population of persistent Bordetella pertussis bacteria. Genetika 52, 422–430.

Laskowski, D., Strzelecki, J., Pawlak, K., Dahm, H., Balter, A., 2018. Effect of ampicillin on adhesive properties of bacteria examined by atomic force microscopy. Micron 112, 84–90. https://doi.org/10.1016/j.micron.2018.05.005.

Lee, C.K., Wang, Y.M., Huang, L.S., Lin, S., 2006. Atomic force microscopy: determination of unbinding force, off rate and energy barrier for protein-ligand interaction. Micron 38 (5), 446–461. https://doi.org/10.1016/j.micron.2006.06.014.

Li, B., Webster, T.J., 2018. Bacteria antibiotic resistance: new challenges and opportunities for implant-associated orthopedic infections. J. Orthop. Res. 36, 22–32. https://doi.org/10.1002/jor.23656.

Li, L., Deng, J., Ma, X., Zhou, K., Meng, Q., Yuan, L., Shi, W., Wang, Q., Li, Y., Yao, K., 2019. High prevalence of macrolide-resistant Bordetella pertussis and ptxP1 genotype, Mainland China, 2014–2016. Emerg. Infect. Dis. 25, 2205–2214. https://doi.org/10.3201/eid2512.181836.

Liu, X., Wang, Z., Zhang, J., Li, F., Luan, Y., Li, H., Li, Y., He, Q., 2018. Pertussis outbreak in a primary school in China: infection and transmission of the macrolide-resistant Bordetella pertussis. Pediatr. Infect. Dis. J. 37, e145–e148. https://doi.org/10.1097/INF.0000000000001814.

Longo, G., Rio, L.M., Roduit, C., Trampuz, A., Bizzini, A., Dietler, G., Kasas, S., 2012. Force volume and stiffness tomography investigation on the dynamics of stiff material under bacterial membranes. J. Mol. Recognit. 25, 278–284. https://doi.org/10.1002/jmr.2171.

Longo, G., Rio, L.M., Trampuz, A., Dietler, G., Bizzini, A., Kasas, S., 2013. Antibiotic-induced modifications of the stiffness of bacterial membranes. J. Microbiol. Methods 93, 80–84. https://doi.org/10.1016/j.mimet.2013.01.022.

Merkel, T.J., Boucher, P.E., Stibitz, S., Grippe, V.K., 2003. Analysis of bvgR expression in Bordetella pertussis. J. Bacteriol. 185, 6902–6912. https://doi.org/10.1128/JB.185.23.6902-6912.2003.

Mishra, M., Parise, G., Jackson, K.D., Wozniak, D.J., Deora, R., 2005. The BvgAS signal transduction system regulates biofilm development in Bordetella. J. Bacteriol. 187, 1474–1484. https://doi.org/10.1128/JB.187.4.1474-1484.2005.

Moon, K., Bonocora, R.P., Kim, D.D., Chen, Q., Wade, J.T., Stibitz, S., Hinton, D.M., 2017. The BvgAS regulon of Bordetella pertussis. mBio 8. https://doi.org/10.1128/mBio.01526-17.

Moreno, N., Chevalier, M., Ronzon, F., Manin, C., Dupuy, M., Krell, T., Rieu, J.-P., 2011. Unbinding forces of single pertussis toxin-antibody complexes measured by atomic force spectroscopy correlate with their dissociation rates determined by surface plasmon resonance. J. Mol. Recognit. 24, 1105–1114. https://doi.org/10.1002/jmr.1159.

Oh, Y.J., Hinterdorfer, P., 2018. Sensing the ultrastructure of bacterial surfaces and their molecular binding forces using AFM. Methods Mol. Biol. 1814, 363–372. https://doi.org/10.1007/978-1-4939-8591-3_21.

Patel, R., 2005. Biofilms and antimicrobial resistance. Clin. Orthop. Relat. Res. 41–47. https://doi.org/10.1097/01.blo.0000175714.68624.74.

Perry, C.C., Weatherly, M., Beale, T., Randriamahefa, A., 2009. Atomic force microscopy study of the antimicrobial activity of aqueous garlic versus ampicillin against Escherichia coli and Staphylococcus aureus. J. Sci. Food Agric. 89, 958–964. https://doi.org/10.1002/jsfa.3538.

Pogoda, K., Piktel, E., Deptuła, P., Savage, P.B., Lekka, M., Bucki, R., 2017. Stiffening of bacteria cells as a first manifestation of bactericidal attack. Micron 101, 95–102. https://doi.org/10.1016/j.micron.2017.06.011.

Relman, D., Tuomanen, E., Falkow, S., Golenbock, D.T., Saukkonen, K., Wright, S.D., 1990. Recognition of a bacterial adhesion by an integrin: macrophage CR3 (alpha M beta 2, CD11b/CD18) binds filamentous hemagglutinin of Bordetella pertussis. Cell 61, 1375–1382. https://doi.org/10.1016/0092-8674(90)90701-f.

Schwesinger, F., Ros, R., Strunz, T., Anselmetti, D., Güntherodt, H.J., Honegger, A., Jermutus, L., Tiefenauer, L., Pluckthun, A., 2000. Unbinding forces of single antibody-antigen complexes correlate with their thermal dissociation rates. Proc. Natl. Acad. Sci. USA 97, 9972–9977. https://doi.org/10.1073/pnas.97.18.9972.

Shahcheraghi, F., Nakhost Lotfi, M., Nikbin, V.S., Shooraj, F., Azizian, R., Parzadeh, M., Allahyar Torkaman, M.R., Zahraei, S.M., 2014. The first macrolide-resistant Bordetella pertussis strains isolated from Iranian patients. Jundishapur J. Microbiol. 7. https://doi.org/10.5812/jjm.10880.

Singh, S., Singh, S.K., Chowdhury, I., Singh, R., 2017. Understanding the mechanism of bacterial biofilms resistance to antimicrobial agents. Open Microbiol. J. 11, 53–62. https://doi.org/10.2174/1874285801711010053.

Stewart, P.S., 2002. Mechanisms of antibiotic resistance in bacterial biofilms. Int. J. Med. Microbiol. 292, 107–113. https://doi.org/10.1078/1438-4221-00196.

Touhami, A., Nysten, B., Dufrêne, Y.F., 2003. Nanoscale mapping of the elasticity of microbial cells by atomic force microscopy. Langmuir 19, 4539–4543. https://doi.org/10.1021/la034136x.

Ventola, C.L., 2015. The antibiotic resistance crisis: Part 1: causes and threats. P T 40, 277–283.

Viljoen, A., Foster, S.J., Fantner, G.E., Hobbs, J.K., Dufrêne, Y.F., 2020. Scratching the surface: bacterial cell envelopes at the nanoscale. mBio 11. https://doi.org/10.1128/mBio.03020-19.

Wang, Z., Cui, Z., Li, Y., Hou, T., Liu, X., Xi, Y., Liu, Y., Li, H., He, Q., 2014. High prevalence of erythromycin-resistant Bordetella pertussis in Xi'an, China. Clin. Microbiol. Infect. 20, O825–O830. https://doi.org/10.1111/1469-0691.12671.

Wang, Z., Li, Y., Hou, T., Liu, X., Liu, Y., Yu, T., Chen, Z., Gao, Y., Li, H., He, Q., 2013. Appearance of macrolide-resistant Bordetella pertussis strains in China. Antimicrob. Agents Chemother. 57, 5193–5194. https://doi.org/10.1128/AAC.01081-13.

Xu, L.C., Siedlecki, C.A., 2009. Atomic force microscopy studies of the initial interactions between fibrinogen and surfaces. Langmuir 25 (6), 3675–3681. https://doi.org/10.1021/la803258h.

Further reading

Scaglione, F., Demartini, G., Dugnani, S., Ferrara, F., Maccarinelli, G., Cocuzza, C., Fraschini, F., 1994. Effect of antibiotics on Bordetella pertussis adhering activity: hypothesis regarding mechanism of action. Chemotherapy 40 (3), 215–220. https://doi.org/10.1159/000239195.

Scarlato, V., Rappuoli, R., 1991. Differential response of the bvg virulence regulon of Bordetella pertussis to MgSO4 modulation. J Bacteriol 173 (22), 7401–7404. https://doi.org/10.1128/jb.173.22.7401-7404.1991.